Strong dependence of dielectric properties on electrical boundary conditions and interfaces in ferroelectric superlattices

I. B. Misirlioglu,[1,a] M. T. Kesim, [2] and S. P. Alpay [2,3]

[1] *Faculty of Engineering and Natural Sciences*
Sabanci University, Tuzla/Orhanli 34956 Istanbul, Turkey
[2] *Department of Materials Science and Engineering and Institute of Materials Science*
University of Connecticut, Storrs, CT 06269 – USA
[3] *Department of Physics*
University of Connecticut, Storrs, CT 06269 – USA

Abstract

A computational study based on Landau-Ginzburg-Devonshire theory is carried out to understand the role of interfaces on the dielectric response of ferroelectric superlattices. Using heteroepitaxial (001)$PbZr_{0.3}Ti_{0.7}O_3$/(001)$SrTiO_3$ heterostructures on (001)$SrTiO_3$ as an example, we show that electrostatic boundary conditions have a pronounced effect on the dielectric response far below the ferroelectric phase transition temperature. For a fixed total multilayer thickness, the average dielectric response can be improved significantly for superlattices with a small layer periodicity. This is due to the large total internal electric fields at the interlayer interfaces which originate from the polarization mismatch between layers.

[a] Corresponding Author, e-mail: burc@sabanciuniv.edu

Adjustment of materials properties via composition in ferroelectric (FE) oxides has become a routine practice due to advancements in thin film deposition techniques. This has triggered further demand from FE and other ferroic oxides as functional/active components in device design. Furthermore, synthesis of artificial superlattices with alternating layer compositions has resulted in the discovery of unconventional properties where the heterostructure has the characteristics of neither of the constituent layers. There exists a vast literature of experimental and theoretical studies that have been carried out to understand and describe the underlying physics in such multicomponent systems and to discover unique properties. [1–27] Only a few of these have consistently tried to explore the dependence of the materials properties of these systems on the number of layers for a given fixed thickness. [5,6,10,13] These have led to the development of detailed theoretical studies based on continuum models [8,9,13,14,18,23,24,26,28] or *ab initio* approaches [7,8,17,29,30] that explicitly focus on the formation of electrical domain structures due to depolarizing/demagnetizing fields resulting from the polarization/magnetization mismatch across the individual layers. The dependence of the FE phase transition temperature T_C and electrical domain stability on the layer configuration near the electrodes has been investigated in a recent analysis. [24] It was found that the transition temperatures and whether the transition from the paraelectric (PE) phase into multi-domain (MD) or single-domain (SD) FE states depends dramatically on the layer configurations near the electrodes, i.e., whether the PE or the FE layer was in contact with the electrodes. It was subsequently shown that assuming periodic boundary conditions in such systems when computing their properties can lead to erroneous conclusions including that the dielectric properties do not depend on superlattice-electrode interfaces but only on the layer thickness. The same factors also apply to the limit of MD-SD stability below the transition temperature as demonstrated in a very recent study. [31]

Despite the amount of research devoted to these systems, dielectric behavior of FE-PE superlattice nanocapacitors still remains controversial. In this study, motivated by the recent theoretical advances [9,13,24,31] we compute the dielectric response of lattice-wise compatible (001) $PbZr_{0.3}Ti_{0.7}O_3/SrTiO_3$ (PZT/STO) superlattices on (001) STO substrates for two different layer configurations. We chose to work with this system as the lattice misfit between PZT and ST is ~1% which can be accommodated without strain relaxation by misfit dislocations up to a film thickness of ~40 nm. This allows us to focus on only coherent interfaces, thereby isolating the effect of internal electric fields resulting from the polarization mismatch between the layers. We employ Landau-Ginzburg-Devonshire theory of FE phase transitions coupled with continuum electrostatic relations to describe properties of PZT/STO heteroepitaxial superlattices as a function of electrical boundary conditions over a wide temperature range. 40 nm thick 8 layer (4 repeating units), 4 layer (2 repeating units) and 2 layer (bilayer) PZT/STO structures having equal layer thickness are considered here with the exception that symmetrical units have half PE layers contacting the electrodes (Fig. 1). We show that the dielectric response of 4 unit structures is significantly larger than 2 unit and bilayer systems both for the bilayer and symmetrical unit structures. We attribute this to the magnitude of the depolarizing fields for small interface periods. This effect is more pronounced in structures with half PE layers contacting the electrodes where the stray fields are strong in the FE layers. Our results indicate that these internal fields can be used as a design parameter for on-chip capacitor and dielectrically tunable device applications.

We consider a 80 × 40 nm grid (*x*- and *z*-axes, respectively) consisting of 0.4 nm cells to ensure proper consideration of domain walls. The superlattice is assumed to be infinite along the *y*-axis, reducing the problem into 2-dimensions. We partition the grid along the *z*-axis via:

$$\Omega = \mathrm{sgn}(\sin\frac{2\pi z}{\lambda}), \qquad (1)$$

$$\text{ferroelectric layer} \rightarrow \text{if } \Omega > 0, \text{ paraelectric layer} \rightarrow \text{if } \Omega < 0, \qquad (2)$$

$$w = 1 \quad \text{if } \Omega > 0 \text{ and } w = 0 \text{ otherwise.} \qquad (3)$$

For the case of the bilayer, z is the vertical position (coordinate) in the superlattice varying from 0 to $n\lambda$ where n is the total number of units, λ is the thickness of the repeating unit. The same approach can be used but this time replacing sine with a cosine function to describe a superlattice with a symmetrical repeating unit (Fig. 1). 1 unit, 2 unit and 4 unit structures (20 nm, 10 nm and 5 nm layer thickness, respectively) are considered both in bilayer and symmetrical unit blocks. Boundaries of FE and PE layers defined by Eqs. (1-3) allow us to write compact equations of state both for the FE and the PE layers as below:

$$\begin{aligned} & w\left\langle \begin{aligned} & 2\alpha_3^m P_z + 4\alpha_{13}^m P_z P_x^2 + 4\alpha_{33}^m P_z^3 + 6\alpha_{111} P_z^5 \\ & + \alpha_{112}(4P_z P_x^4 + 8P_z^3 P_x^2) + 2\alpha_{123} P_z P_x^4 - G\left(\frac{\partial^2 P_z}{\partial z^2} + \frac{\partial^2 P_z}{\partial x^2}\right) \end{aligned} \right\rangle_{FE} \\ & + (1-w)\left\langle 2\alpha_3^m P_z + 4\alpha_{13}^m P_z P_x^2 + 4\alpha_{33}^m P_z^3 - G\left(\frac{\partial^2 P_z}{\partial z^2} + \frac{\partial^2 P_z}{\partial x^2}\right)\right\rangle_{PE} = wE_z + (1-w)E_z \end{aligned}$$

(4a)

$$\begin{aligned} & w\left\langle \begin{aligned} & 2\alpha_1^m P_x + 2(2\alpha_{11}^m + \alpha_{12}^m)P_x^3 + 2\alpha_{13}^m P_x P_z^2 + 6\alpha_{111} P_x^5 + \\ & 2\alpha_{112}[3P_x^5 + 3P_x^3 P_z^2 + P_x P_z^4] + 2\alpha_{123} P_x^3 P_z^2 - G\left(\frac{\partial^2 P_x}{\partial z^2} + \frac{\partial^2 P_x}{\partial x^2}\right) \end{aligned} \right\rangle_{FE} \\ & + (1-w)\left\langle 2\alpha_1^m P_x + 2(2\alpha_{11}^m + \alpha_{12}^m)P_x^3 + 2\alpha_{13}^m P_x P_z^2 - G\left(\frac{\partial^2 P_x}{\partial z^2} + \frac{\partial^2 P_x}{\partial x^2}\right)\right\rangle_{PE} = wE_x + (1-w)E_x \end{aligned}$$

(4b)

The details of the derivation of the above relations were given elsewhere. [32] Here, α_3^m, α_{13}^m, α_{33}^m, α_1^m, α_{11}^m, α_{12}^m are the misfit renormalized dielectric stiffness coefficients of the FE and PE layers[33,34] and take on values of either PZT or ST depending on the value of w, $\alpha = (T - T_C)(2\varepsilon_0 C)^{-1}$ where T_C is the bulk (unconstrained) Curie temperature, and α_{111}, α_{112},

α_{123} are the dielectric stiffness coefficients of the bulk of PZT. The stress-free bulk coefficients of PZT and STO are compiled from Refs. 35 and 36. The superlattices satisfy the Maxwell relation in dielectric media:

$$\nabla \cdot \mathbf{D} = 0 \tag{5}$$

where **D** is the dielectric displacement vector defined through $D_x = \varepsilon_b \varepsilon_0 E_x + P_x$ and $D_z = \varepsilon_b \varepsilon_0 E_z + P_z$, ε_0 is the permittivity of vacuum, ε_b is the background dielectric constant in the FE and PE layers, and P_x and P_z are the *x*- and *z*-components of the total polarization vector. The components of the internal electric field vector are determined from the total electrostatic potential ϕ such that $E_x = -\partial\phi/\partial x$ and $E_z = -\partial\phi/\partial z$. Ideal electrodes are assumed that imply perfect screening of polarization charges at the electrode interfaces to concentrate on the effect of layer periodicity. The polarization boundary conditions for the FE layers are

$$\xi \frac{\partial P_x}{\partial x} - P_x = 0\Big|_{z=-f,+f} \text{ and } \xi \frac{\partial P_z}{\partial z} - P_z = 0\Big|_{z=-f,+f} \tag{6}$$

at the bottom ($z = -f$) and top layer interfaces ($z = +f$) regardless of the type of unit and position with respect to electrodes. We assume that the extrapolation length, ξ, at all interfaces is infinitely large to avoid abrupt changes emanating from finite values of this parameter. Eqs. (4-5) are solved using a Gauss-Seidel iterative scheme in a temperature range 50-800 K at 50 K intervals under a small bias (0.01 V potential drop across the system for Dirichlet boundary conditions) where the initial polarization configuration is a random assignment of ± 0.001 C/m^2 for each cell. We do so to check the stability of the MD state with respect to the SD state and allow the system to choose the stable configuration at any given temperature. Only for very thin layers and low temperatures (<100 K), the MD structure can easily transform into a SD state upon application of the above small bias indicating the proximity of the energies of the two

configurations. Our results indicate that for the 5 nm, 10 nm and 20 nm individual layer thicknesses, the MD state is stable below the FE-PE transition temperatures for each type of superlattice considered in the current study.

In Fig. 2, we provide the average of the absolute value of out of plane polarization $<|P_z|>$ for the systems considered in Fig. 1. Tracking $<|P_z|>$ is the only way here to detect the phase transitions because the FE layers in the thickness range considered here are in a MD state. A SD state at low temperatures can be stabilized at some layer thickness below 1 nm for the bilayer and below 2 nm for the symmetrical unit under the small bias mentioned above owing to the relatively large in-plane dielectric constant for this system, favoring domain formation even for such layer thicknesses. This is because the in-plane dielectric constant of PZT 30:70 on STO is rather high, ranging from 120-140 around RT to 300 or slightly higher near T_C, making MD formation quite easy, and possibly leaving little room for SD stability. The sudden slope changes in the evolution of the $<|P_z|>$ in the bilayer structures are due to the strain-induced stabilization of P_x in the FE layers. Such behavior is not observed in the symmetrical unit structures as they have both P_z and P_x components getting stabilized together at T_C.

Following the numerical data provided in Fig. 2 from which the T_C can be found, we can compare our results to those obtainable from analytical theory that has yielded consistent results for the $BaTiO_3$/STO and $KTaO_3$/$KNbO_3$ systems earlier. [9,24] Briefly, in that approach, the linear equation of state for a FE-PE superlattice with the FE layer in a uniaxial polar state is solved along with the appropriate equations of electrostatics in charge free media and we adapt the same method for our structures here. The comparative results are provided in Fig. 3. Our simulation results here follow closely the curve obtained for PZT/STO bilayer and symmetrical unit derived from analytical theory wherein an approximate linear dielectric constant of STO was assumed.

The deviation of our results from analytical theory is due to the fact that we consider all polarization terms, and more importantly, the temperature dependent in-plane polarizability of both PZT and STO way reach high values leading to deviations from analytical theory. The transition temperatures (and the amplitude of polarization obtained in our study) in the system are reduced with increasing number of units (reduced layer thickness) for both bilayer and symmetrical units. T_C for the symmetrical unit structures are lower than the bilayer structures since the FE layers are not in contact with the electrodes. [24] The transition starts from the FE in contact with one of the electrodes for the bilayer while it is homogeneous in the superlattice with symmetrical units for fixed total layer thickness. In fact, the transition is always homogeneous for superlattices consisting of symmetrical units regardless of thickness. [24] The sudden slope change in Fig. 2 around 550 and 300 K for the 10 nm and 5 nm bilayers, respectively, is due to the stabilization of the in-plane polarization in the PZT layers via strain while the finite values of in-plane polarization above this temperature are due to closure type domains originating from polarization rotations near the interfaces and domain walls. The symmetrical unit structures do not display such a behavior as the P_x components stabilized by strain appear spontaneously along with P_z.

The rather interesting outcome of such transition behavior is reflected in the dielectric response of the structures shown in Fig. 4. We compute the dielectric response along the out of plane direction via $\varepsilon_r = (1/\varepsilon_0)d < P_z > / dE_z$. It is seen that the thick layers (one unit and two units) transforming into a MD state at their respective T_C have no anomaly and the superlattices of both types (consisting of bilayers and symmetrical units) with 4 units have a reduced T_C, broad but finite dielectric curve with an anomaly-like behavior. This reveals the impact of interfaces on such structures along with reduced unit layer thickness. The structures consisting of 4

symmetrical units have a higher dielectric response overall because the transition is homogeneous. Unlike the superlattice with 4 symmetrical units, the swelling of the anomaly-like dielectric response for 4 unit bilayer structure corresponds to the occurrence of the strain-stabilized in-plane components of polarization as mentioned above (not shown here). On the other hand, the peak observed in the superlattice consisting of 4 symmetrical units exactly corresponds to the transition [compare Figs. 2(b) and 4(b)]. For the 2 and 1 unit superlattices consisting of either symmetrical or bilayer units, domains are more stable against an applied field (compared to the 4 unit superlattices), yielding no anomaly-like features at the transition into the MD state but only a slope change at T_C is evident. Note that superlattices with 1 and 2 units of either type have similar dielectric response values in the range of temperatures considered here. All structures, when far above their T_C's have also identical dielectric response – a qualitatively expected outcome of our simulations. At higher temperatures, the dielectric response of all structures converge to the same value (ε_R~500). Using the linear equation of state, $a_3^m P_Z = 2V_{FE}/h$ and $V_{FE} + V_{PE} = V$ (V is the small voltage signal) in the FE and PE layers for a bilayer, we obtain:

$$\varepsilon_{FE} = \frac{2\varepsilon_{PE}}{\varepsilon_0(\varepsilon_b + \varepsilon_{PE})}\left(a_3^m + \frac{1}{\varepsilon_0(\varepsilon_b + \varepsilon_{PE})}\right)^{-1}, \qquad (7)$$

for the PE state of the FE layers where ε_{PE} is the linear dielectric response of the STO layer computed at relevant temperatures. This yields a value of ~500 around 900 K in the limit far from T_C for all structures and gradually decreases to ~420 at 1000 K, in excellent agreement with the numerical solution (Fig. 3). The situation below T_C in the presence of domains in alternating layers is not so straightforward and is obtained as shown here numerically. Eq. (7) is also valid for the structure consisting of symmetrical units in the PE phase. We note that Eq. (7) is obtained for a single unit and might deviate from values for very large systems in the bilayer case due to

the inhomogeneous nature of the polarization amplitude in the layers. Furthermore, the values of the dielectric permittivity we obtain indicate that the strongest response comes from the FE layers.

In summary, using a nonlinear thermodynamic model taking into account the electrical and mechanical boundary conditions, we show that there is a strong dependence of the layer thickness and the layer configuration with respect to the electrodes on the dielectric properties of FE-PE superlattices, in particular for the polar state below the T_C. Convergence of the dielectric response of all structures to the same value in the high temperature limit is expected and confirmed. Decreasing individual layer thickness and thus increasing the number of interfaces yields the largest dielectric response from the structures described in this study and stands out as an important parameter in device design. This response is even more enhanced if PE layers are contact with the top and bottom electrodes. Thus, in addition to layer thickness, choice of the layers contacting the electrodes can be used as an effective design parameter in utilizing such structures for device applications. While our work considers the thermodynamic near-equilibrium results, hence the quasi-static dielectric response, we are tempted to think that the thinner layer structures with reduced T_C due to repeating interfaces at short periods might be expected to operate more effectively with values close to what is given in this work at MHz to lower limit GHz frequencies of ac bias which device applications often target.[37] Therefore, localized periodic depolarizing fields occuring at the PZT/STO interfaces of thin units in MD state might allow a better dielectric response and tunability under ac bias. This effect might be more prominent particularly in symmetrical unit superlattices due to overall reduced T_C with respect to those composed of bilayer units.

Acknowledgements

IBM acknowledges the support of Turkish Academy of Sciences (TÜBA) GEBİP. The authors would also like to thank A. P. Levanyuk for stimulating comments on the data.

REFERENCES

[1] R.E. Camley and D.R. Tilley, Phys. Rev. B **37**, 3413 (1988).

[2] D. Schwenk, F. Fishman, and F. Schwabl, J. Phys. Condens. Matter **2**, 5409 (1990).

[3] K. Iijima, T. Terashima, Y. Bando, K. Kamigaki, and H. Terauchi, J. Appl. Phys. **72**, 2840 (1992).

[4] H. Tabata, H. Tanaka, and T. Kawai, Appl. Phys. Lett. **65**, 1970 (1994).

[5] E.D. Specht, H.-M. Christen, D.P. Norton, and L.A. Boatner, Phys. Rev. Lett. **80**, 4317 (1998).

[6] H.-M. Christen, E.D. Specht, D.P. Norton, M.F. Chisholm, and L.A. Boatner, Appl. Phys. Lett. **72**, 2535 (1998).

[7] J.B. Neaton and K.M. Rabe, Appl. Phys. Lett. **82**, 1586 (2003).

[8] W. Tian, J.C. Jiang, X.Q. Pan, J.H. Haeni, Y.L. Li, L.Q. Chen, D.G. Schlom, J.B. Neaton, K.M. Rabe, and Q.X. Jia, Appl. Phys. Lett. **89**, 092905 (2006).

[9] V.A. Stephanovich, I.A. Luk'yanchuk, and M.G. Karkut, Phys. Rev. Lett. **94**, 047601 (2005).

[10] D.A. Tenne, A. Bruchhausen, N.D. Lanzillotti-Kimura, A. Fainstein, R.S. Katiyar, A. Cantarero, A. Soukiassian, V. Vaithyanathan, J.H. Haeni, W. Tian, D.G. Schlom, K.J. Choi, D.M. Kim, C.B. Eom, H.P. Sun, X.Q. Pan, Y.L. Li, L.Q. Chen, Q.X. Jia, S.M. Nakhmanson, K.M. Rabe, and X.X. Xi, Science (80-.). **313**, 1614 (2006).

[11] D.G. Schlom, L.Q. Chen, C.B. Eom, K.M. Rabe, K.S. Streiffer, and J.M. Triscone, Annu. Rev. Mater. Res. **37**, 589 (2007).

[12] Y.L. Li, S.Y. Hu, D. Tenne, A. Soukiassian, D.G. Schlom, L.Q. Chen, X.X. Xi, K.J. Choi, C.B. Eom, A. Saxena, T. Lookman, and Q.X. Jia, Appl. Phys. Lett. **91**, 252904 (2007).

[13] Y.L. Li, S.Y. Hu, D. Tenne, A. Soukiassian, D.G. Schlom, X.X. Xi, K.J. Choi, C.B. Eom, A. Saxena, T. Lookman, Q.X. Jia, and L.Q. Chen, Appl. Phys. Lett. **91**, 112914 (2007).

[14] I.B. Misirlioglu, G. Akcay, S. Zhong, and S.P. Alpay, J. Appl. Phys. **101**, 036107 (2007).

[15] I.B. Misirlioglu, M. Alexe, L. Pintilie, and D. Hesse, Appl. Phys. Lett. **91**, 022911 (2007).

[16] A. Soukiassian, W. Tian, V. Vaithyanathan, J.H. Haeni, L.Q. Chen, X.X. Xi, D.G. Schlom, D.A. Tenne, H.P. Sun, X.Q. Pan, K.J. Choi, C.B. Eom, Y.L. Li, Q.X. Jia, C. Constantin, R.M. Feenstra, M. Bernhagen, P. Reiche, and R. Uecker, J. Mater. Res. **23**, 1417 (2008).

[17] X. Wu, K.M. Rabe, and D. Vanderbilt, Phys. Rev. B **83**, 020104 (2011).

[18] N.A. Pertsev, P.E. Janolin, J.-M. Kiat, and Y. Uesu, Phys. Rev. B **81**, 144118 (2010).

[19] K. Kathan-Galipeau, P. Wu, Y. Li, L.-Q. Chen, A. Soukiassian, X. Xi, D.G. Schlom, and D.A. Bonnell, ACS Nano **5**, 640 (2011).

[20] K. Kathan-Galipeau, P.P. Wu, Y.L. Li, L.Q. Chen, A. Soukiassian, Y. Zhu, D.A. Muller, X.X. Xi, D.G. Schlom, and D.A. Bonnell, J. Appl. Phys. **112**, 052011 (2012).

[21] J.Y. Jo, P. Chen, R.J. Sichel, S.J. Callori, J. Sinsheimer, E.M. Dufresne, M. Dawber, and P.G. Evans, Phys. Rev. Lett. **107**, 055501 (2011).

[22] P. Chen, M.P. Cosgriff, Q. Zhang, S.J. Callori, B.W. Adams, E.M. Dufresne, M. Dawber, and P.G. Evans, Phys. Rev. Lett. **110**, 047601 (2013).

[23] A.L. Roytburd, S. Zhong, and S.P. Alpay, Appl. Phys. Lett. **87**, 092902 (2005).

[24] A.P. Levanyuk and I.B. Misirlioglu, J. Appl. Phys. **110**, 114109 (2011).

[25] M.B. Okatan, J. Mantese, and S. P. Alpay, Phys. Rev. B **79**, 174113 (2009).

[26] F.A. Urtiev, V.G. Kukhar, and N.A. Pertsev, Appl. Phys. Lett. **90**, 252910 (2007).

[27] M. Liu, C. Ma, G. Collins, J. Liu, C. Chen, A.D. Alemayehu, G. Subramanyam, Y. Ding, J. Chen, C. Dai, Y. Lin, and M.W. Cole, Nanoscale Res. Lett. **8**, 338 (2013).

[28] D.R. Tilley, Solid State Commun. **65**, 657 (1988).

[29] X. Wu, O. Diéguez, K.M. Rabe, and D. Vanderbilt, Phys. Rev. Lett. **97**, 107602 (2006).

[30] X. Wu, M. Stengel, K.M. Rabe, and D. Vanderbilt, Phys. Rev. Lett. **101**, 087601 (2008).

[31] A.P. Levanyuk and I.B. Misirlioglu, Appl. Phys. Lett. **103**, 192906 (2013).

[32] I.B. Misirlioglu, H.N. Cologlu, and M. Yildiz, J. Appl. Phys. **111**, 064105 (2012).

[33] N.A. Pertsev, A.G. Zembilgotov, and A.K. Tagantsev, Phys. Rev. Lett. **80**, 1988 (1998).

[34] N.A. Pertsev, V. Kukhar, H. Kohlstedt, and R. Waser, Phys. Rev. B **67**, 054107 (2003).

[35] M.J. Haun, Z.Q. Zhuang, E. Furman, S.J. Jang, and L.E. Cross, Ferroelectrics **99**, 45 (1989).

[36] N.A. Pertsev, A.K. Tagantsev, and N. Setter, Phys. Rev. B **61**, R825 (2000).

[37] G. Subramanyam, M. W. Cole, N. X. Sun, T. S. Kalkur, N. M. Sbrockey, G. S. Tompa, X. Guo, C. Chen, S. P. Alpay, G. A. Rossetti, Jr., K. Dayal, L. Q. Chen and D. G. Schlom, J. Appl. Phys. 114, 191301 (2013).

FIGURE CAPTIONS

Figure 1: Schematics of various 40 nm-thick PZT/STO heterostructures on STO considered in this study. (a) a bilayer and (b) a symmetrical heteroepitaxial multilayer configuration with periodicities of n=1, 2, and 4 corresponding to a repeating unit thickness h= 40, 20, and 10 nm respectively.

Figure 2: (Color online) Average absolute value of out of plane polarization $<|P_z|>$ for 40 nm-thick PZT/STO heterostructures with n=1, 2, and 4 repeating unit(s) on STO for (a) bilayer and (b) symmetrical repeating unit systems.

Figure 3: (Color online) T_C of PZT/STO heterostructures on STO as a function of single layer thickness (h/2) in a repeating bilayer and symmetrical unit obtained numerically in this work (simulated) and from analytical theory.

Figure 4. (Color online) Temperature dependent dielectric response of 40 nm-thick PZT/STO heterostructures on STO with n=1, 2, and 4 repeating unit(s) consisting of (a) bilayer and (b) symmetrical units.

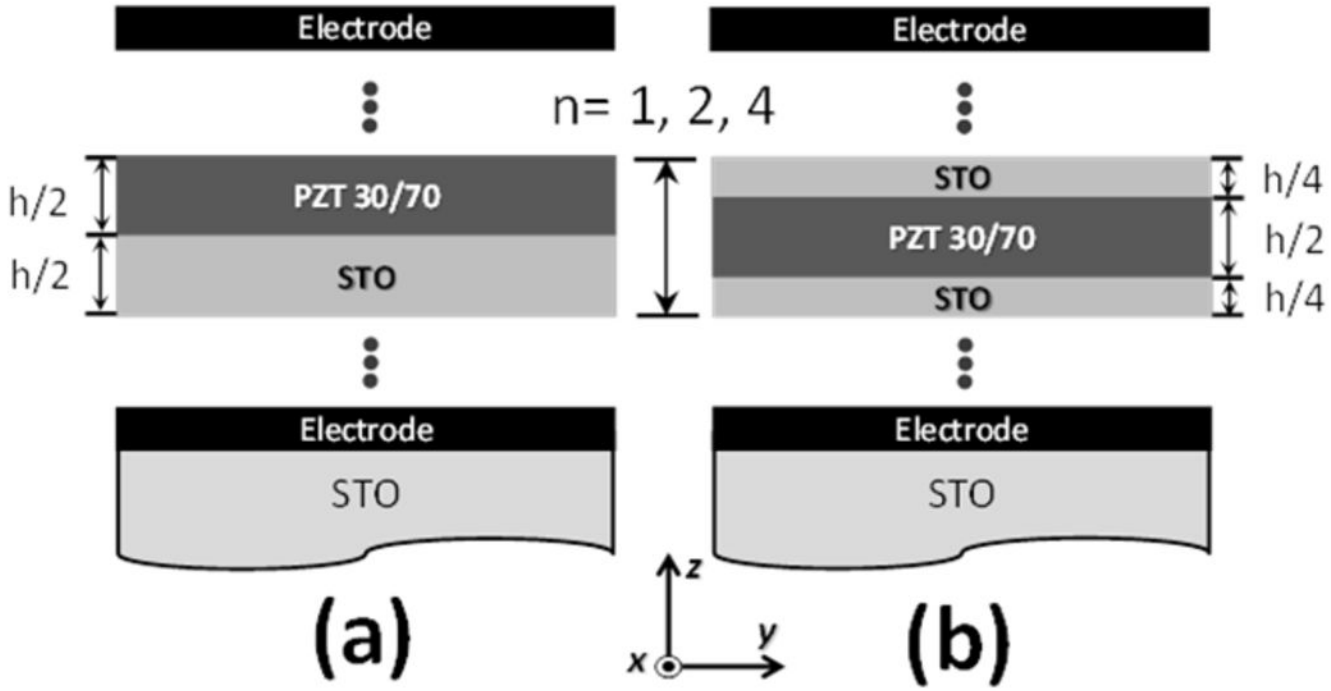
Electrode
Electrode
n= 1, 2, 4
h/2
h/2
PZT 30/70
STO
STO
PZT 30/70
STO
h/4
h/2
h/4
Electrode
Electrode
STO
STO
z
x
y
(a)
(b)

Figure 1

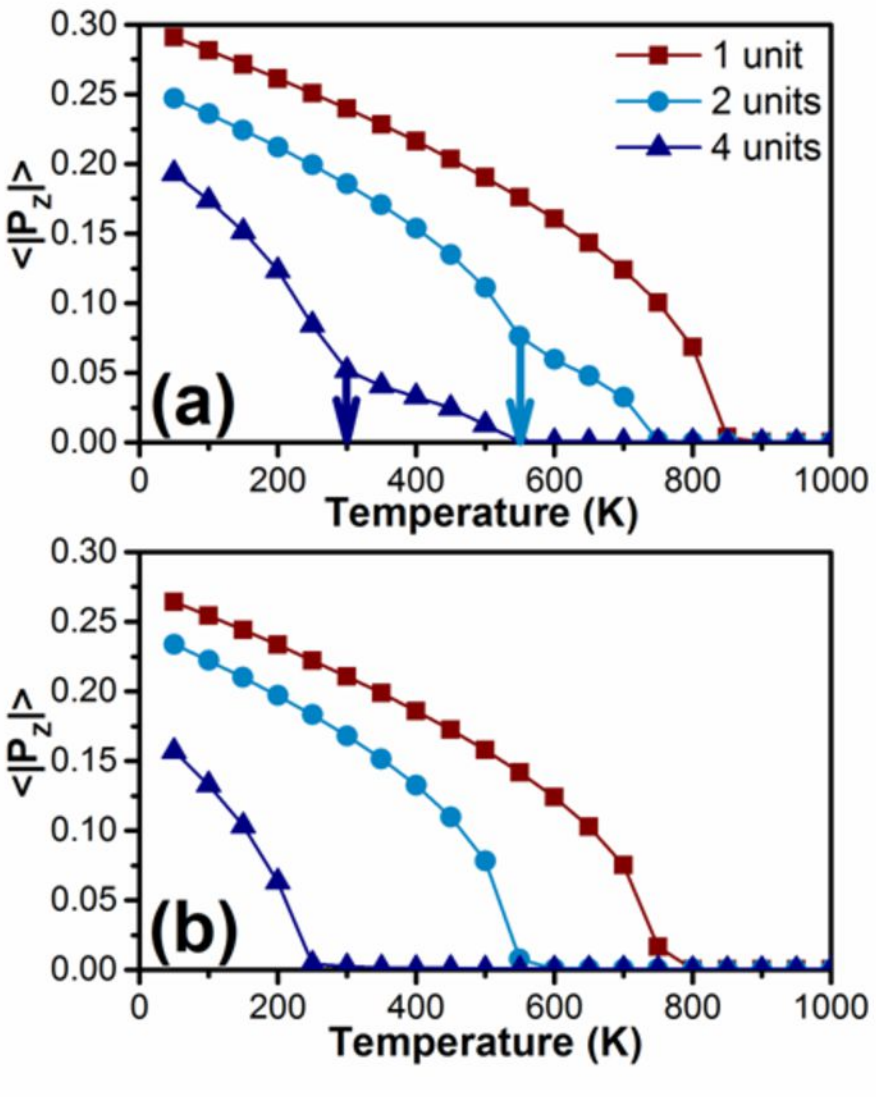
0.30
0.25
0.20
0.15
0.10
0.05
0.00
<|Pz|>
1 unit
2 units
4 units
(a)
0
200
400
600
800
1000
Temperature (K)
(b)

Figure 2

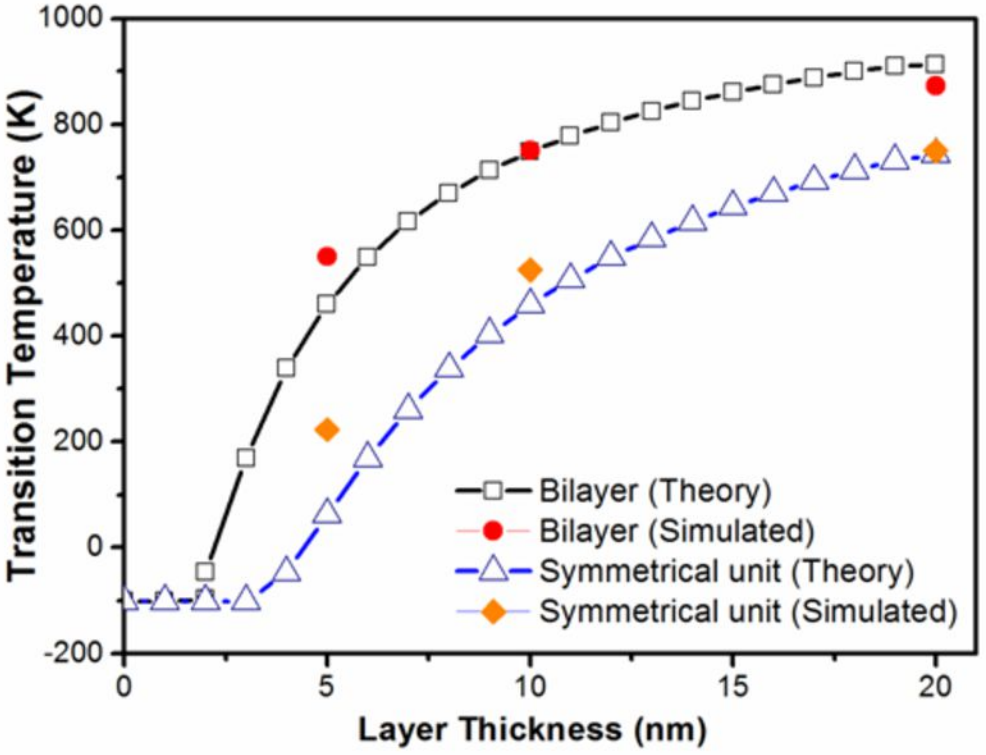
Transition Temperature (K)
1000
800
600
400
200
0
-200
0
5
10
15
20
Layer Thickness (nm)
Bilayer (Theory)
Bilayer (Simulated)
Symmetrical unit (Theory)
Symmetrical unit (Simulated)

Figure 3

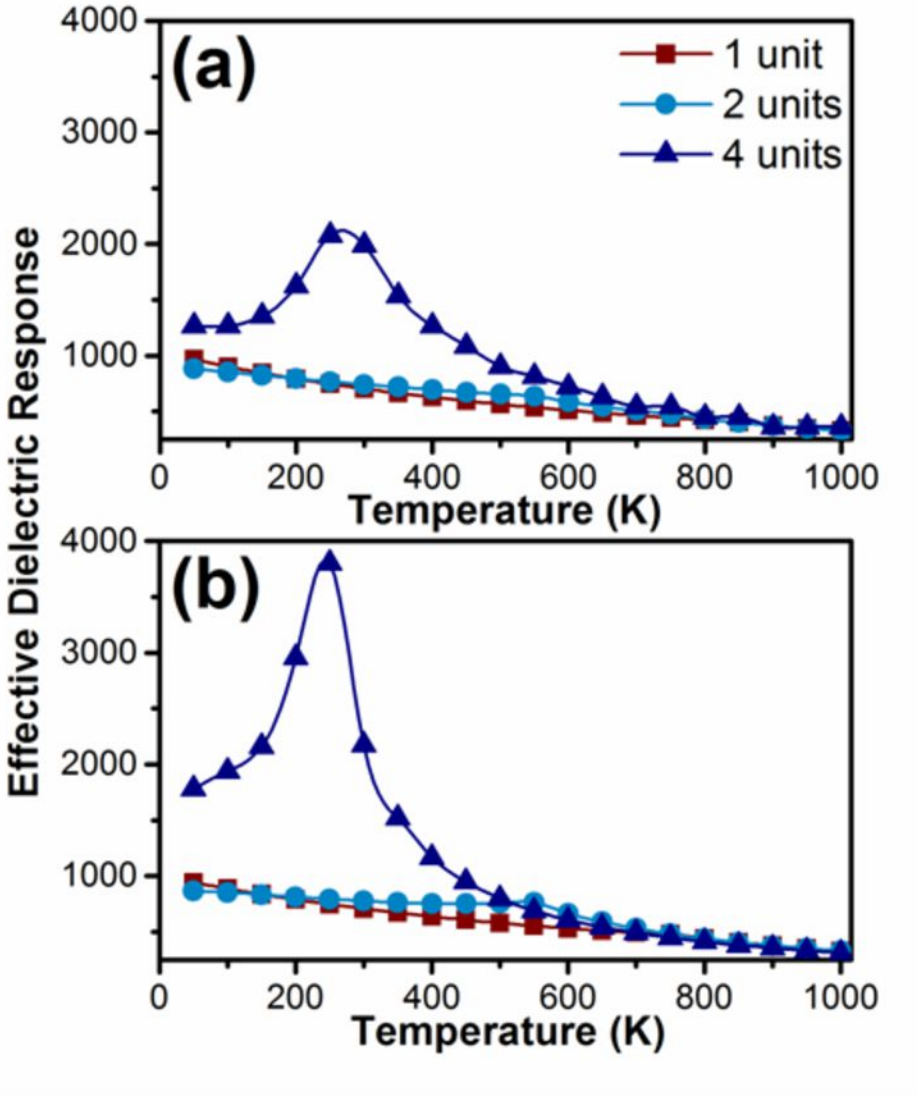
(a)
1 unit
2 units
4 units
Effective Dielectric Response
Temperature (K)
(b)
Temperature (K)
4000
3000
2000
1000
0
200
400
600
800
1000

Figure 4